Molecular Systems Biology (2006) doi:10.1038/msb4100081

www.molecularsystemsbiology.com
Article number: 41

molecular systems biology

Noise in transcription negative feedback loops: simulation and experimental analysis

Yann Dublanche[1], Konstantinos Michalodimitrakis[1], Nico Kümmerer, Mathilde Foglierini and Luis Serrano*

European Molecular Biology Laboratory (EMBL), Heildelberg, Germany
* Corresponding author. European Molecular Biology Laboratory (EMBL), SCB, Meyerhofstrasse 1, 69117 Heildelberg, Germany.
Tel.: +49 6 221387320; Fax: +49 6 221387306; E-mail: serrano@embl.de
[1] These authors contributed equally to this work

Received 11.1.06; accepted 14.6.06

Negative feedback loops have been invoked as a way to control and decrease transcriptional noise. Here, we have built three circuits to test the effect of negative feedback loops on transcriptional noise of an autoregulated gene encoding a transcription factor (TF) and a downstream gene (DG), regulated by this TF. Experimental analysis shows that self-repression decreases noise compared to expression from a non-regulated promoter. Interestingly enough, we find that noise minimization by negative feedback loop is optimal within a range of repression strength. Repression values outside this range result in noise increase producing a U-shaped behaviour. This behaviour is the result of external noise probably arising from plasmid fluctuations as shown by simulation of the network. Regarding the target gene of a self-repressed TF (sTF), we find a strong decrease of noise when repression by the sTF is strong and a higher degree of noise anti-correlation between sTF and its target. Simulations of the circuits indicate that the main source of noise in these circuits could come from plasmid variation and therefore that negative feedback loops play an important role in suppressing both external and internal noise. An important observation is that DG expression without negative feedback exhibits bimodality at intermediate TF repression values. This bimodal behaviour seems to be the result of external noise as it can only be found in those simulations that include plasmid variation.
Molecular Systems Biology 1 August 2006; doi:10.1038/msb4100081
Subject Categories: synthetic biology; simulation and data analysis
Keywords: autoregulation; negative feedback loop; noise; SmartCell; TetR

Introduction

The genetic programme of a cell and/or an organism is determined by a complex web of gene and protein networks. Taking into account the small number of some of the components in the networks (especially in transcription processes), it is surprising that in general cells and organisms manage to carry out this programme in a reproducible way. How the cell copes with the noise, or even in some cases uses it for its advantage (Chen *et al*, 2005), is a fascinating topic that has prompted many groups to analyse it theoretically (Kepler and Elston, 2001; Swain *et al*, 2002; Paulsson, 2004; Austin *et al*, 2006) and experimentally (Becskei and Serrano, 2000; Elowitz *et al*, 2002; Ozbudak *et al*, 2002; Swain *et al*, 2002; Blake *et al*, 2003; Raser and O'Shea, 2004; Chen *et al*, 2005; Hooshangi *et al*, 2005; Pedraza and van Oudenaarden, 2005; Austin *et al*, 2006). In principle, there are two sources of noise that could affect transcriptional networks: intrinsic and extrinsic (Swain *et al*, 2002; Paulsson, 2004). Although the definition of both is somehow relative (Paulsson, 2004), we could in principle define intrinsic noise as that arising directly from the circuit and external as that due to changes in the surrounding environment. For example, intrinsic noise could be due to the randomness in the binding of the polymerase to the promoter of one of the network genes and external could be due to fluctuations in the activity of the polymerase owing to changes in the metabolic status of the cell. Elegant experiments have been carried out by different groups to try to separate one type of noise from the other (Swain *et al*, 2002), to determine the sources of noise (Ozbudak *et al*, 2002; Blake *et al*, 2003), as well as to study cascade noise amplification in a network (Hooshangi *et al*, 2005; Pedraza and van Oudenaarden, 2005). One way in which cells could suppress noise is by using negative feedback loops (Savageau, 1974). Experimental study of a designed negative feedback loop in *Escherichia coli* showed how introduction of negative feedback decreased noise level (Becskei and Serrano, 2000; Austin *et al*, 2006), explaining its high frequency in prokaryotic organisms (Thieffry *et al*, 1998).

Recently, Paulsson (2004) published a thorough theoretical analysis of noise in gene networks and presented an equation that decomposes the intrinsic and extrinsic noise contributions, simplifying its analysis. Based on this equation, the author analysed the experimental negative feedback circuit described by Becskei and Serrano (2000). The results suggested that the noise in the circuit analysed by the authors

should mainly come from fluctuations in plasmid numbers and the suppression of the noise by the negative feedback loop should be mainly owing to elimination of the fluctuations introduced by changes in the plasmid number. This would suggest that negative feedback loops do not suppress intrinsic noise, but rather eliminate external noise that might arise for example from plasmid variation, or other external sources of noise like ribosome variation (Austin *et al*, 2006). In a recent work, it has also been shown that negative feedback shifts noise to higher frequencies characteristic of intrinsic noise, while filtering external noise (Austin *et al*, 2006).

To see if this is the case, we have reproduced the original experiment of Becskei and Serrano (2000) using a more sensitive approach to quantify GFP expression (FACS sorting versus microscopy used in the previous work). Also we have created new constructs in which the reporter protein (GFP) is no more fused to the Tet repressor (TetR) but rather regulated by TetR. In this way, we can analyse the effect of noise suppression of a negative feedback loop on a downstream gene and compare it with that found in a gene transcription cascade with no feedback (Hooshangi *et al*, 2005; Pedraza and van Oudenaarden, 2005). Three constructions have been analysed: (a) TetR fused to GFP and repressing itself (TG-nf); (b) TetR repressing itself and GFP, with the latter being expressed from a different promoter (T + G-nf); and (c) TetR expressed by a constitutive promoter and repressing GFP (T + G) (Figure 1). To reproduce the normal situation in a prokaryotic cell, we have used a low-copy plasmid for TetR (around four copies) and a medium-copy plasmid (around 60 copies) for the GFP reporter. In this way, we reproduce the fact that many negatively regulated transcription factors in *E. coli* regulate several downstream genes. In parallel, we have carried out a detailed stochastic simulation of the networks taking into account cell division, plasmid variation and competition of other promoters for the polymerase. Simulations have been carried out with the SmartCell software (http://smartcell.embl.de/) (Ander *et al*, 2004) that uses the Gillespie (1977) algorithm as modified by Gibson and Bruck (2000) and Stundzia and Lumsden (1996) to include space and diffusion. This new version of SmartCell uses the modification of Elf and co-workers (Hattne *et al*, 2005) to accelerate calculations (http://smartcell.embl.de/).

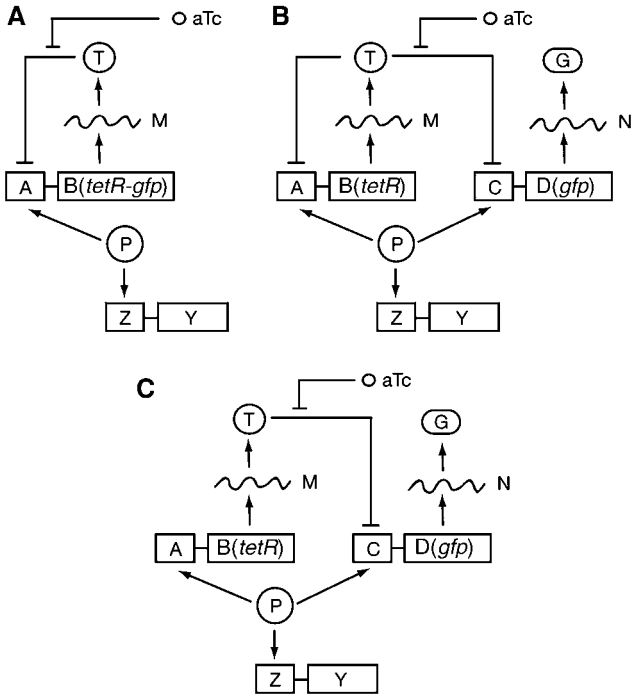

Figure 1 Schematic diagram of the three circuits analysed in this work. (**A**) Negative feedback loop where the TetR protein is fused to GFP (TG-nf) on a low copy plasmid (~4 copies). (**B**) Negative feedback loop, where TetR represses itself and also production of GFP (T + G-nf). TetR is located in a low-copy plasmid (~4 copies) and the reporter on a medium-copy plasmid (~60 copies). (**C**) TetR is constitutively produced and represses GFP production. TetR is located in a low-copy plasmid (~4 copies) and the reporter on a medium-copy plasmid (~60 copies). The circles represent the protein produced: T for TetR, G for GFP and P for polymerase. Promoters are shown as squares: A for the TetR promoter and its regulatory region, C for the GFP promoter and its regulatory region and Z for all other promoters in *E. coli* that could compete for the polymerase. RNA is shown as a wavy line. Arrows mean activation and line ended lines inhibition.

Results

Experimental analysis of GFP expression in the different circuits

The three different circuits shown in Figure 1 were analysed under different concentrations of anhydrotetracycline hydrochloride (aTc) ranging from 0 to 100 ng/ml. This range was chosen on the following basis: the amount of TetR produced by the constitutive promoter is smaller than that produced in DH5αZ1 cells and 100 ng/ml of aTc has been shown to fully titrate TetR in the latter case (Lutz and Bujard, 1997). Specifically, the amount of TetR produced by the constitutive promoter was estimated by Western blotting (as explained in Materials and methods) to be approximately 2500 molecules when using DH5αZ1 cells as reference, which have approximately 7000 molecules of TetR dimer per cell (Lutz and Bujard, 1997). Although ideally the state where the promoter is completely free of repression should be analysed with cells carrying only the GFP-expressing plasmid, this was not possible because in the complete absence of TetR, the TetR-regulated promoter, $P_{LtetO-1}$, at least in this strain (Top10) and under the given experimental conditions, readily undergoes a recombination event, which destroys the promoter (data not shown). After addition of aTc at the desired concentration, cells were grown for 2.5 h (or 3 h) at 37°C and then analysed using the FACS sorter to look at the distribution of fluorescent cells. In Figure 2D, we show the results of a typical experiment for the three circuits and for Top10 cells without any plasmid as a control. In the case of the TetR-GFP fusion, we see a low amount of overall fluorescence even at close to saturation concentrations of aTc (Figures 2D and 3A), as expected owing to the lower copy number of the plasmid expressing TetR-GFP (3–4 copies) compared to that expressing GFP alone (50–70 copies). In the absence of aTc, the levels of TetR-GFP are barely detectable (also verified by Western blotting (data not shown)). It should be pointed out that although the level of TetR-GFP is barely detectable in the absence of aTc, it is sufficient to ensure stability of the promoter, as all cells are

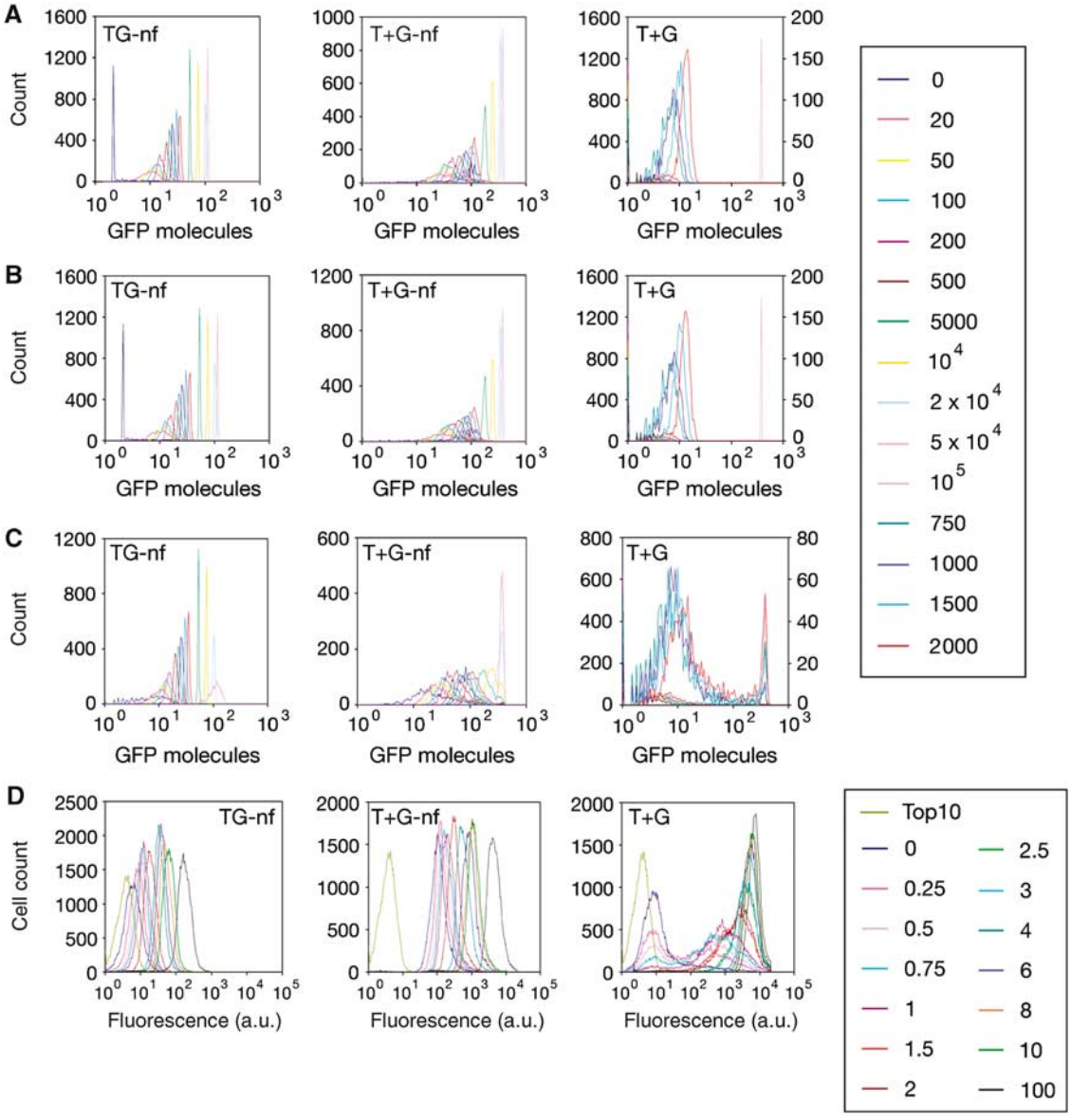

Figure 2 FACS analysis and simulation-derived histograms of the three circuits under different aTc concentrations. (**A**–**C**) Simulation-derived histograms for the circuits for different numbers of aTc molecules with constant plasmid copy number (A), variable polymerase levels (B) and variable plasmid copy number (C). In all three cases, the values for circuit T + G for 750, 1000, 1500 and 2500 aTc molecules have been plotted on a secondary *Y*-axis for clarity and the respective legend entries are at the bottom of the legend to separate them from the others. (**D**) FACS analysis of the three circuits for different aTc concentrations (in ng/ml). Cells with no plasmids (Top10) were used as a control for the level of autofluorescence.

responsive to the increase of aTc. In the case of GFP under the control of TetR, we find similar final amounts of fluorescence for the case in which TetR represses itself and in that in which TetR is not involved in a negative feedback loop (Figures 2D and 3A; it should be noted that the two figures correspond to different experiments). This appears to be in qualitative agreement with the simulations (Figure 3B). However, the response to aTc is very different in the two cases (Figure 2D). In the negative feedback loop circuit, we observe a very homogeneous distribution of GFP in the cell population that gradually moves from a low fluorescence value to higher ones with increasing aTc concentration. In the other case, we see a complicated behaviour in which at intermediate aTc values fluorescence of cells spans several orders of magnitude, whereas some cells seem not to express GFP at all. Only at high and very low aTc values, we see a single population. Another interesting feature is the 'ease' with which the two circuits reach the state corresponding to saturation: although the negative feedback circuit starts with a barely detectable level of TetR, it requires a higher dose of aTc to reach saturation, compared to the non-regulated circuit, which reaches GFP saturation very quickly. This can be explained when considering the fact that in the case of the negative feedback loop, addition of aTc could be subjected to a type of 'buffering' effect: aTc can relieve temporarily autorepression, leading to higher expression of TetR until TetR levels are such

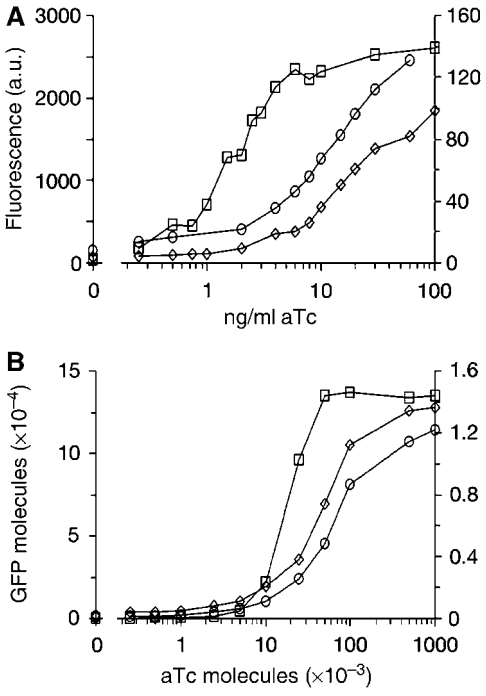

Figure 3 Experimental and theoretical changes in fluorescence with increasing amounts of aTc. (**A**) Mean fluorescence values measured by FACS for the TG-nf circuit (○), the T + G-nf circuit (◇) and T + G circuit (□). (**B**) Number of GFP molecules calculated with the simulations for the TG-nf circuit (○), the T + G-nf circuit (◇) and T + G circuit (□). In both cases, values for the TG-nf circuit are plotted on a secondary *Y*-axis for clarity.

that the loop can be restored in the presence of the given aTc concentration.

Noise analysis in the experimental circuits

To compare the level of noise in the three circuits, we used the V_c (coefficient of variance determined by dividing the standard deviation by the mean; see Materials and methods) values. This value gives an indication of the spread of the population with respect to the mean. The higher the V_c value is, the more noisy is the system. In Figure 4D, we show the plots of the change in V_c with respect to aTc concentration for the three circuits for four different experiments; three were conducted for 2.5 h and one for 3 h. Comparing the results obtained with the three circuits, the first obvious conclusion is that all of them arrive to similar V_c values (around 0.5 ± 0.1) at high aTc concentrations where there is no repression by TetR. Second, we can observe that the V_c values are very high for the T + G circuit (Figure 4D, right) at low aTc concentrations where TetR still represses the GFP promoter. For the negative feedback (T + G-nf), we find intermediate values at low aTc values (Figure 4D, centre). In the case of the TG-nf circuit (Figure 4D, left), we find that noise is slightly larger at very low aTc concentration, then decreases when increasing aTc and finally goes up again at high aTc concentration (the large V_c value at 0 aTc could be partly due to intrinsic autofluorescence of the *E. coli* cells; see below). This behaviour is different from previous published work (Becskei and Serrano, 2000), as it was indicated that the noise of the TG-nf circuit simply increased with the amount of aTc. Here, we have found that at very low aTc, the noise is as high as at very high aTc and it decreases at slightly higher aTc concentrations. This discrepancy can be explained if we consider that light microscopy was used to analyse the noise in the original paper and thus very low values of aTc could not be explored. Here, by using FACS sorting, we have been able to explore very low aTc values. Another reason for the discrepancy could lie in the sampling of cells for calculating V_c values. In the absence of aTc for the TG-nf circuit, the level of GFP expression is so low that the distribution greatly overlaps with the autofluorescence distribution of Top10 cells. Although this means that the V_c value will not represent accurately the levels of GFP, it will still reflect the profile of the entire population, as it is including even the non-expressing or very low-expressing cells.

Simulation analysis of the three circuits

To get a better understanding of the mechanisms behind the different behaviour of the three circuits with respect to GFP expression and V_c values, we have made a detailed model of the three circuits (see Materials and methods). In this model, we consider fluctuations owing to binding of the polymerase to competing promoters in the cell, the possibility of having more than one polymerase per gene/operon at the same time and binding of aTc to the free and bound TetR at the two binding sites (see Figure 5 for all reactions being considered). The values used for the simulation have been obtained from experimental data when available (Table I). As simulations covered time periods (1 day=86 400 s) much longer than that of the *E. coli* cell cycle compared to the 30 min cell division time experimentally measured for the given growth conditions, it was necessary to limit the lifetime of the species used in the simulation in order to capture the real changes in their concentration owing to cell division. Thus, a pseudo-degradation rate was given to such components, so that they have an apparent half-life corresponding to the measured cell division time. The circuits have been simulated using the software SmartCell (Ander *et al*, 2004).

The first runs, using values previously published in literature for half-lives, promoter strengths, etc., resulted in too high values for the final concentrations of TetR and GFP. Thus, we slightly altered the degradation rates of TetR and GFP in order to have approximately the same final numbers of molecules as found in this study (similar results were obtained if instead we slightly modified the production rates). Regarding aTc concentration, it is very difficult to make equivalence between experimental values and the ones used for simulation. The reason is that in the case of the negative feedback loop, the aTc concentration inside an *E. coli* cell could be much higher than in the medium, due to a sink effect of TetR binding to aTc. Specifically, owing to the strong binding of aTc to TetR (Degenkolb *et al*, 1991), molecules of aTc that enter the cell will readily bind to TetR, resulting, on the one hand, in de-repression and production of more TetR and, on the other, depletion of free aTc molecules inside the cell. The latter would be the driving force for more aTc molecules to diffuse from the medium into the cell, increasing the total amount of aTc (free and bound) inside the cell compared to that of the medium.

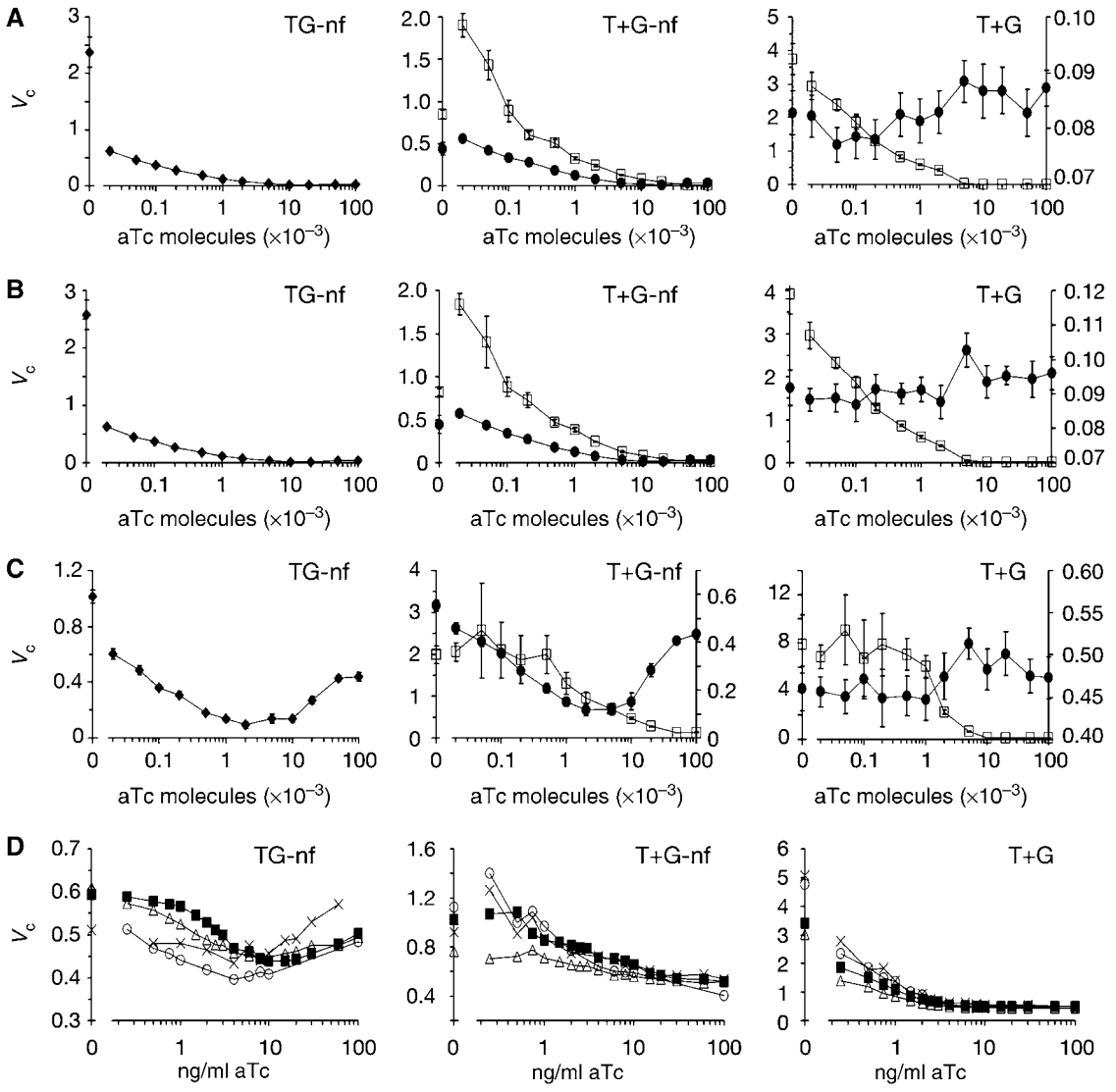

Figure 4 Changes in V_c values for the three circuits with increasing amounts of aTc, obtained from simulation and experiments. (A–C) Simulation results. (**A**) No plasmid variation. (**B**) Polymerase random variation. (**C**) Plasmid variation. On each row, the first plot corresponds to the TG-nf circuit showing the changes in V_c for the fusion TetR-GFP (◆), the second to the T + G-nf circuit and the third to the T + G circuit, showing the changes in V_c for TetR (●) and GFP (□). Values for TetR for the T + G circuit have been plotted on a secondary *Y*-axis. (**D**) Experimental results. Four different experiments are shown with one of them being conducted for 3 h (■) instead of 2.5 h as with the rest. The V_c value was determined using the following equation: V_c=Standard deviation/mean.

Comparison between experimental and simulated data

We have run three different types of simulations (see Figure 5 for the reactions considered) to see the effect of external and internal noise. In the first case, we simulated the three circuits with a fixed number of plasmids and polymerase. In the second case, we allowed for variation in the number of polymerase molecules by changing degradation and production rates within reasonable values (see Materials and methods). Finally, we considered the possibility of variation in the number of plasmids per cell using the values described in the literature.

Comparison between the experimental and simulated values for the expression of GFP shows that the behaviour of TG-nf and T + G-nf is well captured by the simulation (Figure 2) independently of the conditions considered (polymerase variation, plasmid number variation or only internal noise). However, for the circuit without negative feedback (T + G), only in the case of plasmid variation (Figure 2C) we see a good fitting to the experimental data (Figure 2D), with a bimodal distribution at intermediate aTc concentrations.

In Figure 4, we show the V_c values as calculated from the simulations of the three circuits (no external noise (Figure 4A), varying polymerase concentration (Figure 4B) and varying plasmid number (Figure 4C), the experimental data (Figure 4D)). In this case, we could see that only when considering plasmid variation we can observe a good fitting to the experimental data for the TG-nf circuit. Regarding the T + G-nf circuit, we could see a marginally better reproduction

Table I Parameters used in the simulations

Initial amount Species	Number of particles	Concentration (mol/l)
P	3600	7.4714E−05
A	4	8.3015E−08
C	60	1.2452E−06
Z	870	1.8056E−05

Reaction rate Name	Value	Name	Value
k_{on_A}	6.7E + 08 M^{-1} s^{-1} with nf	k_{off_C}	0.025 s^{-1}
k_{on_A}	6.7E + 07 M^{-1} s^{-1} without nf	k_{deg_N}	0.005 s^{-1}
k_{off_A}	0.025 s^{-1}	k_{on_Ta1}	7.40E + 06 M^{-1} s^{-1}
k_{in}	0.3 s^{-1}	k_{off_Ta1}	3.70E−05 s^{-1}
$k_{transcr}$	0.133 s^{-1}	k_{on_Ta2}	3.70E + 06 M^{-1} s^{-1}
$k_{transcr2}$	0.06	k_{off_Ta2}	7.40E−05 s^{-1}
$k_{translM}$	0.09 s^{-1}	k_{on_T6}	1.00E + 06 M^{-1} s^{-1}
$k_{translN}$	0.1	k_{off_T6}	1.00E−05 s^{-1}
k_{deg_M}	0.005 s^{-1}	k_{on_T7}	1.00E + 06 M^{-1} s^{-1}
k_{on_Z}	6.70E + 08	k_{off_T7}	1.00E−03 s^{-1}
k_{off_Z}	0.025	k_{on_T8}	1.00E + 06 M^{-1} s^{-1}
k_{on_T1}	1.00E + 06 M^{-1} s^{-1}	k_{off_T8}	100 s^{-1}
k_{off_T1}	1.00E−05 s^{-1}	k_{on_T9}	7.40E + 06 M^{-1} s^{-1}
k_{on_T2}	1.00E + 06 M^{-1} s^{-1}	k_{off_T9}	3.70E−05 s^{-1}
k_{off_T2}	1.00E−03 s^{-1}	k_{on_T10}	3.70E + 06 M^{-1} s^{-1}
k_{on_T3}	1.00E + 06 M^{-1} s^{-1}	k_{off_T10}	7.40E−05 s^{-1}
k_{off_T3}	100 s^{-1}	k_{deg_G}	1.74E−03 s^{-1}
k_{on_T4}	7.40E + 06 M^{-1} s^{-1}	k_{prod_A}	5.50E−04 s^{-1}
k_{off_T4}	3.70E−05 s^{-1}	k_{deg_A}	1.38E−04 s^{-1}
k_{on_T5}	3.70E + 06 M^{-1} s^{-1}	k_{prod_C}	2.78E−03 s^{-1}
k_{off_T5}	7.40E−05 s^{-1}	k_{deg_C}	4.63E−05 s^{-1}
k_{deg_T}	1.16E−03 s^{-1}	k_{prod_P}	1.668 s^{-1}
k_{on_C}	6.70E + 08 M^{-1} s^{-1}	k_{deg_P}	4.63E−04 s^{-1}

nf stands for negative feedback loop.

of the behaviour with plasmid variation (observe the plateau for V_c at low aTc concentrations in Figure 4C and D that is missing in Figure 4A and B). For the T + G circuit, introduction of plasmid variation seems to make the fitting to the experimental data worse. However, we should consider the very large standard deviation for the simulated and experimental circuits at very low aTc concentrations. Moreover, as mentioned above, introduction of plasmid variation is necessary to capture the observed bimodality in the T + G circuit. Thus, the simulations point to plasmid variation as one of the major sources of external noise.

Although experimentally we have not followed the V_c for TetR in the T + G-nf and T + G networks, simulations show a similar U-shaped behaviour for TetR in the T + G-nf as in the TG-nf circuit (data not shown) and as expected a constant V_c value for the T + G circuit (no autorepression of TetR). Interestingly, the V_c values for the simulated TG-nf circuit are lower at 0 aTc with plasmid variation than under the two other conditions. The reason for this is that at very low aTc when we introduced plasmid variation the average level of TetR increases, probably because the basal level of TetR is very low (around 10 molecules with no plasmid variation). Thus, any random increase in plasmid number has a good chance of allowing one or more rounds of transcription before the TetR level goes high enough to repress these extra copies. As a result, the V_c is smaller, which seems contradictory. The same reasoning could also explain the U-shaped profile of the V_c–aTc curve (see Discussion).

We also examined the importance of having a medium-copy plasmid with the reporter gene by repeating the simulations with low-copy plasmids and allowing for plasmid variation. Analysis of the relationship between V_c and aTc shows exactly the same behaviour as above (data not shown).

Correlated noise and negative feedback loop

To quantify the expression fluctuations and the degree of correlation between TetR and GFP genes in the T + G-nf and in the T + G circuits, we computed the correlation parameter C_{ij} as described by Pedraza and van Oudenaarden (2005), using the computer simulation data considering plasmid variation (Figure 6A). In the case of the T + G circuit, we see a behaviour similar to that described by Pedraza and van Oudenaarden (2005) for genes 1 and 2 in their gene cascade. Essentially at low aTc, the noise in GFP expression does not correlate with the noise in TetR. At higher aTc concentrations, there is a negative correlation between both protein products, so that noise in GFP expression decreases with the amount of active TetR product. Finally, at high aTc, we see again an uncoupling of the noise in both proteins. However, the behaviour for the T + G-nf circuit is different. In this case, we see a larger negative correlation from the beginning, indicating a much higher coupling between the two systems. At intermediate aTc concentrations, this coupling is maximal and more than double than that seen in the T + G circuit.

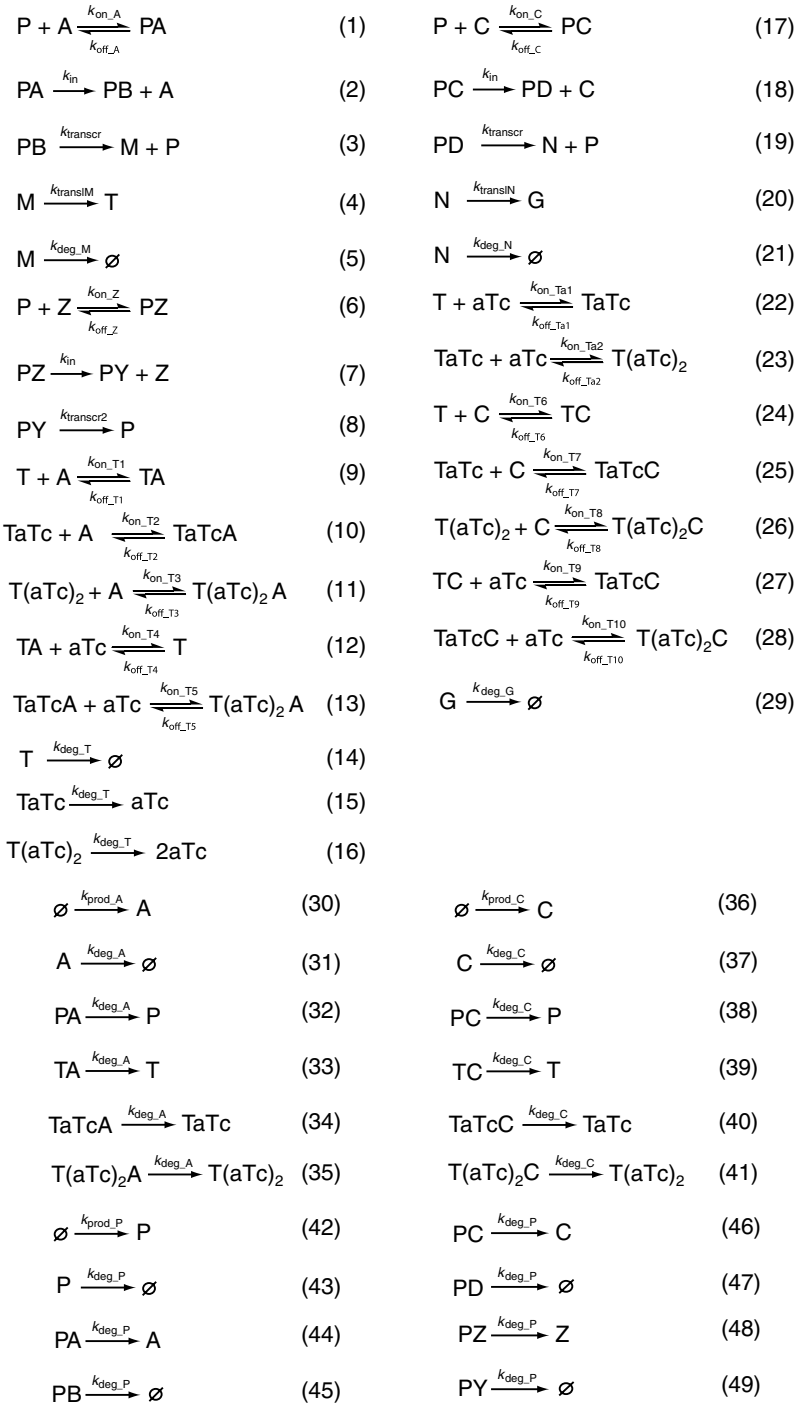

Figure 5 Summary of all the reactions considered in the SmartCell simulation of the three circuits. P is the RNA polymerase, T is TetR protein, G is GFP protein, aTc is anhydrotetracycline, A is the activator part of the plasmid expressing TetR, PA is the RNA polymerase–activator A complex on the respective plasmid, PB is the complex of the RNA polymerase with the TetR gene, C is the activator part of the plasmid expressing GFP, PC is the RNA polymerase–activator C complex on the respective plasmid, PD is the complex of the RNA polymerase with the GFP gene, Z is the chromosomal *E. coli* promoters, PZ is the RNA polymerase–chromosomal promoter complex, PY is the complex of the RNA polymerase with chromosomal *E. coli* genes, M is TetR mRNA, N is GFP mRNA, TaTc, TaTcA and TaTcC are the complexes of free TetR or DNA-bound TetR and one molecule of aTc, $T(aTc)_2$, $T(aTc)_2A$ and $T(aTc)_2C$ are the complexes of free TetR or DNA-bound TetR and two molecules of aTc, TA is the TetR–activator A complex and TC is the TetR–activator C complex.

Noise frequency and negative feedback loops

In a recent paper, it was shown that negative feedback regulation in a gene results in a shift of the noise frequency towards high frequencies when compared to a non-regulated gene (Austin *et al*, 2006). To see if this was the case in our simulated circuits, we calculated the noise frequency (see Materials and methods). We did this for the TG-nf and T + G-nf

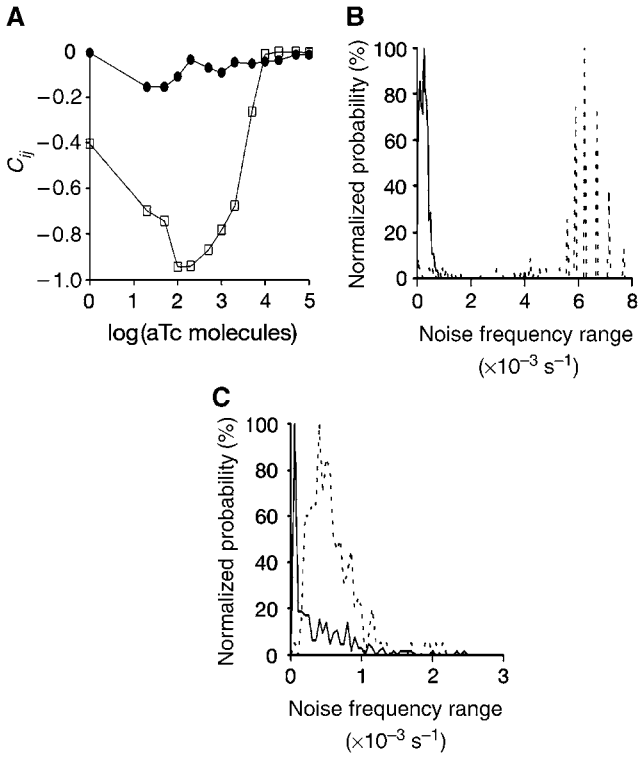

Figure 6 Correlation between the expression levels of TetR and GFP in the negative feedback circuit and in the non-regulated one and effect of negative autoregulation on noise frequency range. (**A**) (□) T + G-nf circuit. (●) T + G circuit. The correlation coefficient was determined using the following equation (Pedraza and van Oudenaarden, 2005): $C_{ij}=(|F_iF_j|-|F_i||F_j|)/(|F_i||F_j|)$. Where the | | symbols denote averaging over all cells in the population and the indices *i* and *j* refer to the repressor and reporter genes, respectively. (**B**) Model of the shift of the noise frequency range distribution owing to negative feedback when compared to a non-regulated gene. The continuous line represents the distribution for the TG-nf circuit in the presence of high aTc when TetR does not regulate anymore the expression of GFP. The dotted line represents the distribution at low aTc, when the negative feedback loop is operational. (**C**) Model of the shift of the noise frequency range distribution of the downstream gene in the T + G-nf circuit when TetR is not regulated (high aTc, continuous line) or is negatively autoregulated (low aTc, dotted line). Low aTc corresponds to 2000 and high to 50 000 aTc molecules.

circuits at the aTc concentration where V_c of TetR was lower and at high aTc where repression does not take place anymore. The results of this analysis are shown in Figure 6B and C. As previously found, negative feedback shifts noise frequency to higher values when compared to a non-regulated gene in both cases. However, the frequency shift is larger for the TG-nf circuit (Figure 6B) than for the T + G-nf (Figure 6C).

Discussion

In this work, we have analysed experimentally and computationally the noise in a negative feedback-regulated transcription factor, as well as the effect the negative feedback loop has on a gene repressed by the same transcription factor.

Noise and bimodality

One of the interesting results we have obtained is the existence of a bimodal behaviour in the expression of GFP in the T + G network at intermediate aTc concentrations. This bimodality could only be reproduced in our simulations when considering plasmid variation. Bimodal behaviour has been described in positive feedback loops (Becskei *et al*, 2001) and in switches (Gardner *et al*, 2000). However, to our knowledge, no bimodal behaviour has been attributed to the combination of a particular circuit (in this case repression by a transcription factor) and a source of external noise. Thus, our result suggests that noise contribution to circuit behaviour could be very important and should be taken into account. Also, this result supports the hypothesis that plasmid variation is one of the major sources of external noise in our circuits.

Noise behaviour and repression

We observed that for all cases the presence of a negative feedback loop decreases significantly the noise in the production of the GFP protein compared to the non-regulated circuit, at aTc concentrations that still allow repression. However for TetR, it places the optimum level of noise suppression at intermediate aTc concentrations. Under conditions where repression is too tight, the TetR noise level is similar to the totally unrepressed circuit. A simpler explanation for this behaviour is the following: although the negative feedback loop suppresses noise, at low aTc concentrations the base noise level is higher under these conditions owing to low TetR-GFP fusion protein population. Thus, a random increase in plasmid number has a good chance of allowing one or more rounds of transcription before the TetR level goes high enough to repress these extra copies. Increasing the aTc concentration reduces the base noise level by increasing expression levels (as seen in the T + G circuit). However, at the same time it disrupts the feedback loop, leading to an increase in noise or decrease of the circuit's noise-suppressing ability. The final result of these two opposing phenomena is a U-shaped behaviour. This means that noise is minimized at intermediate levels of repression. At higher levels of repression, noise increases owing to low protein population, whereas the negative feedback suppression of noise decreases at lower levels of repression.

Regarding the non-repressed circuit, we see an immediate decrease of noise the moment some aTc is added to the medium. This contradicts the behaviour observed by other groups for non-regulated networks. In the case of Pedraza and van Oudenaarden (2005), they observed a plateau followed by a decrease in noise at high IPTG concentrations. Other groups like Elowitz *et al* (2002) or Hooshangi *et al* (2005) observed a hump in the noise at medium IPTG (Elowitz *et al*, 2002) or aTc (Hooshangi *et al*, 2005) concentrations and smaller V_c values (maximum around 1, whereas we obtained values around 3–4). In the case of Hooshangi *et al* (2005), this hump was not predicted to happen in the simulation of their circuit for a one-stage cascade circuit. In fact their simulation showed a very similar behaviour to the one observed in our work. At this point, it is difficult to determine the reason behind these differences. The fact that simulations using Gillespie-based approximations showed similar behaviours for one-stage cascade (Hooshangi *et al*, 2005) could suggest that discrepancies could be due to sensitivity problems in the low expression range of fluorescent proteins. In fact when looking at Figure 2

it is clear that for 0 aTc in the TG-nf and T + G circuits, there is a significant overlap between cell autofluorescence and GFP expression. One could argue that a correction for this factor should be introduced so that V_c reflects only the GFP-expressing cells. However, we would argue that as long as the overlapping is not 100%, no correction should be made. Otherwise, we will eliminate the noise component due to cells that do not express GFP when others do, as seen in the bimodal distribution for the T + G circuit. Thus, as long as the overlapping between autofluorescent cells and cells induced with aTc is not 100%, we should consider the V_c values. In any case, even when eliminating the first two points for the TG-nf circuit, we will still have a U-shaped behaviour.

Negative feedback loop and transfer of information

Calculation of the cross-correlation parameter C_{ij} between the TetR and the downstream GFP-regulated gene shows a stronger negative coupling between TetR levels and GFP levels when there is a negative feedback loop (around four times). This means that a negative feedback loop not only decreases the noise of the transcription factor autorepressing itself, but also increases significantly the transfer of information to the downstream gene, which ultimately will be the desired biological trait of any circuit.

In a recent work (Simpson *et al*, 2003; Austin *et al*, 2006), it has been proposed that negative feedback loops shift noise frequency from low to high values when compared with non-regulated circuits. The authors proposed that this frequency shift may have biological relevance, as higher-frequency noise is more easily filtered out by downstream gene circuits in a regulatory cascade, and therefore has little regulatory impact. Analysis of noise frequency on our simulation data considering external source coming from plasmid variation shows this kind of behaviour for GFP when comparing the T + G-nf circuit at high aTc concentration (no regulation) and at medium aTc concentration (strong self-regulation and low V_c) (Figure 6C). Similar results are also found for the TG-nf circuit (Figure 6B), indicating that the shift in frequency takes place at the level of the self-repressed gene as well as its target. The only difference is that the shift is larger in the case of the TG-nf circuit.

Noise origins

Simulation of the three circuits, using a model of the transcription regulation in *E. coli*, as well as empirical parameters, shows a good agreement between experimental observations and the predicted behaviour when plasmid variation is taken into account. Thus, for the TG-nf circuit, we could really see the U-shaped behaviour for the noise. For the T + G-nf and T + G circuits, simulations show higher noise for the latter. Regarding GFP expression, we saw how simulations reproduced the experimental data showing some kind of bistability for the non-regulated T + G circuit and a smooth transition from low to high expression for the other two circuits. These results are independent of plasmid number, as similar results are obtained with medium and low copy numbers for the reporter gene (data not shown).

The advantage of the simulation is that it allows one to test different sources of noise in the system, which when compared with the experimental data allows to discriminate the more probable ones. Our results clearly indicate that as suggested by Paulsson (2004) plasmid variation upon cell division could be the most probable source of noise on the circuits analysed here. However, we cannot rule out other sources of external noise contributing as well. Polymerase variation could be one of those but our data indicate that at least within what one could expect to be the natural variation this will not be a likely cause. Other mechanisms like metabolic status, variation in ribosome numbers (Austin *et al*, 2006), access to the promoter, etc. could also contribute. In a recent paper (Austin *et al*, 2006) analysing noise in a negative feedback circuit, the authors found that aTc alone could have a strong influence on the noise of a non-regulated circuit. They proposed that binding of aTc to ribosomes and inhibition of translation could be an important external noise source. However, previous literature indicated that aTc has some toxic effects in *E. coli* at very high concentrations (>1 μg/ml and not ng/ml) through interference with the cell membrane but not through ribosome binding (Oliva *et al*, 1992). In any case, it seems that intrinsic noise of the system alone cannot explain the experimental observations and that external noise produced for example by plasmid variation is filtered by the negative feedback loop. Although it is not the case here, prokaryotic cells could use other mechanisms to diminish noise than negative feedback loops. One of them is DNA looping (Vilar and Saiz, 2005). In DNA looping, a repressor or activator binds to DNA at the promoter site and at the same time to a distal site on DNA. As a result, a repressor could release the binding site near the promoter allowing transcription while still bound to the distal site and this in turn allows faster re-binding and repression compared to a free repressor. The outcome then is equivalent to a faster k_{on} for the repressor and therefore to noise decrease.

Materials and methods

Experimental analysis

Materials

Ampicillin, kanamycin and aTc were purchased from Sigma. For Western blotting, the primary antibody was a mixture of two monoclonal mouse antibodies for TetR from MoBiTec and the secondary antibody was peroxidase-conjugated donkey anti-mouse, from Jackson ImmunoReasearch Laboratories. Bands were visualized by the ECL Western blotting analysis kit from Amersham Biosciences.

Bacterial strains and plasmids

The strain used for cloning and experiments is Top10 from Invitrogen (*F*$^-$ *mcr*A Δ(*mrr-hsd*RMS-*mcr*BC) φ80*lac*ZΔM15 Δ*lac*X74 *deo*R *rec*A1 *ara*D139 Δ(*ara-leu*)7697 *gal*U *gal*K *rps*L (Str^R) *end*A1 *nup*G). Only for the construction of pZEmG (see below), XL10-Gold cells, from Stratagene, were used. Plasmids pZE21-MCS-1, pZE12-Luc and pZS*24-MCS-1 (Lutz and Bujard, 1997) were used as starting material to construct vectors carrying the constructs. A monomeric form of GFP was cloned into pZE21-MCS-1 with *Kpn*I–*Bam*HI, resulting in plasmid pZEmG. This GFP variant is GFPmut3.1 with the A206K mutation (Zacharias *et al*, 2002), which was introduced by PCR using the forward primer CACACAATCTaaaCTTTCGAAAGATCCCAACGAAAAG AGAGAC and the reverse primer CTTTCGAAAGtttAGATTGTGTGGACA GGTAATGGTTGTCTGG. The kanamycin resistance gene of pZS*24-MCS-1 was exchanged with the ampicillin resistance gene of pZE12-Luc by *Aat*II–*Sac*I digestion, yielding plasmid pZS*14-MCS-1. The $P_{lac/ara-1}$ promoter of pZS*14-MCS-1 plasmid was exchanged with

the $P_{LtetO-1}$ promoter of pZE21-MCS-1 by digestion with *Aat*II and *Kpn*I, resulting in plasmid pZS*11-MCS-1. TetR from Tn10 was cloned into pZS*14-MCS-1 and pZS*11-MCS-1, yielding plasmids pZS*14T (non-regulated TetR expression) and pZS*11T (TetR negative feedback loop), respectively. A *Bam*HI site was placed before the stop codon of the *tetR* gene. This site was used to introduce the gene of the monomeric GFP in pZS*11T, resulting in plasmid pZS*11TG, which expresses the fusion protein TetR-GFP.

Bacterial growth

Bacteria were grown at 37°C, in LB containing the appropriate antibiotics to ensure plasmid propagation, inoculating directly from glycerol stocks. The overnight cultures were used to inoculate 1:100 fresh LB medium containing antibiotics and the desired amount of aTc and grown for 2.5 or 3 h at 37°C. Comparison of the behaviour of the three circuits analysed at these two growth times did not show any significant difference, indicating that the system has reached steady state.

Flow cytometry analysis

One millilitre of cells, prepared as described above, was harvested and re-suspended in 2 ml of filtered PBS (0.22 μm filter). Cells without GFP were always used as a control to establish the level of autofluorescence. The analysis was performed on a DAKO MoFlo Flow Cytometer (DakoCytomation GmbH, Hamburger Strasse 181,22083, Hamburg). The laser power used was 1.2 W of 488 nm light. This has an added benefit of near saturating the GFP on the sorter. Approximate measurement of fluorochrome saturation was performed by increasing the light until no more increase in fluorescent signal was seen.

Oscilloscope set-up

Channel 1 on the oscilloscope had a BNC T splitter fitted. On the DOT Plot board, the signal sent to channel 1 of the oscilloscope was set to 2 (SSC—see above). The T splitter feeds the signal from the Dot Plot board to the input channel 1 of the oscilloscope and, via an additional length of BNC cable, to the trigger board. The SSC amplifier was switched to LOG mode to enable LOG signal triggering. The SSC signal was thresholded while the sample was running by adjusting the threshold rotary knob until the bacterial population was revealed on the scatter plots. The sample rate was approximately 2000–5000 events/s. The differential pressure was low to confine the bacteria to the centre of the co-axial flow. The data were analysed using DOKOCytomation Summit software.

Quantification of TetR

Cells were grown as described above, harvested, re-suspended in water, lysed by boiling with Laemmli buffer for 10 min and analysed by SDS–PAGE, followed by Western blotting. After transfer, all proteins on the membranes were visualized by Ponceau staining, and then the membranes were scanned with Agfa Duoscan *f*40 scanner. The stain was subsequently removed by washing with PBS. The membranes were blocked at room temperature for 1 h with 5% milk in PBST (PBS containing 0.05% Tween 20) and then exposed to the primary antibody for 1 h at room temperature and to the secondary antibody for 45 min. Each step with an antibody was followed by two 10 min washes with PBST. After the final wash, TetR bands were visualized with ECL and the exposed films were scanned. Using the program IQMac, the number of pixels for each band on the film was determined and then divided by the number of pixels from the total protein stain of the corresponding lane. Both values were first corrected for background (by subtracting the number of pixels of membrane/film corresponding to the same area as the lane/band) to adjust for differences in the amount of protein transferred in each lane. The value for the bands of TetR from DH5αZ1 cells was used as a reference to calculate the concentration of TetR in cells carrying pZS*14T and pZS*11T.

Simulation

Basis of SmartCell

SmartCell, a software written in C++, is designed for modelling biological processes occurring in a cell (Ander *et al*, 2004). The simulation environment is divided into elementary divisions, called 'voxels', to localize events and species. Two groups of voxels can be defined: (1) the compartment, limited by a membrane, is used to define an area with particular properties, and (2) the region is only used to localize reactions or initial amounts. In each voxel, the species can be represented by the concentration or the number of particles. Two types of events exist in SmartCell, diffusion events, representing the movements of species in one compartment or between two compartments, and chemical reactions. At the end of the simulation, two types of output presenting the evolution of species during time are created, the SUM files, representing the evolution in a compartment, and the VOXEL files, representing the evolution in each voxel.

There are two easy-to-use interfaces, available to use SmartCell. First, the graphic user interface facilitates the writing and design of the biological model. Second, an output analysis tool gives an easier and faster way to analyse a huge amount of outputs.

The executable version of SmartCell is freely available on the web page of SmartCell project, held at EMBL: http://smartcell.embl.de.

Improvements of SmartCell algorithm

The version of SmartCell presented in the SmartCell Paper (Ander *et al*, 2004) was based on the next event algorithm, using Gibson and Bruck's (2000) optimization of the Gillespie algorithm. The most important aspect of this algorithm is the use of one event queue to sort the events that can happen during the simulation. All events are duplicated as many times as the number of voxels where it may occur. The next subvolume method (Elf *et al*, 2003; Elf and Ehrenberg, 2004) is an alternative to the next event algorithm. For this method, the program uses only one queue, with a size equal to the number of voxels. This queue is sorted with the time when the next event will occur in each voxel. As explained in MesoRD papers (Elf *et al*, 2003; Elf and Ehrenberg, 2004), the next reaction algorithm could be complementary to that of the next event and, consequently, SmartCell now proposes both algorithms.

Noise determination

We have run each simulation 200 times for each circuit and condition. As there is no correlation between two time points separated by 10 000 s, we have extracted several values from each run. For the V_c, we have taken values at times 40 000, 60 000 and 80 000 s. For the histograms of GFP, we have taken values at times 20 000, 30 000, 40 000, 50 000, 60 000, 70 000 and 80 000 s. For the networks with low copy number, we have made 100 runs and we have taken values at times 40 000, 60 000 and 80 000 s.

The noise frequency analysis was performed using the normalized autocorrelation functions as described by Austin *et al* (2006), using a sampling interval T_s of 10 s. The noise frequency range F_n was found using $F_n=1/\tau_{1/2}$, where $\tau_{1/2}$ was the value of τ where the normalized autocorrelations function reached a value of 1/2. The normalized autocorrelation function is defined by

$$\mathrm{ACF_m}(jT_s) = \frac{\frac{\sum_{n=1}^{N-j} X_m(nT_s)X_m((n+j)T_s)}{N-j} - [X_m]^2}{\frac{\sum_{n=1}^{N} X_m^2(nT_s)}{N} - [X_m]^2}$$

where X_m is the copy number function, $[X_m]$ the mean value of the X_m function and T_s the sampling interval (here 10 s). A graph of normalized probability of noise frequency was finally made using a binning of 0.5×10^{-4}.

Description of the networks

Three related networks involving TetR and GFP in an *E. coli* cell are modelled. In all networks, competition of RNA polymerase binding to the promoter in the plasmids for chromosomal promoters is modelled assuming that all chromosomal promoters have the same properties

and are thus represented by a single species (Z). The number of Z was assumed to be 870 based on the fact that this is approximately the number of genes/operons expressed simultaneously in *E. coli* (Selinger *et al*, 2000). The networks are schematically shown in Figure 1 and the reactions describing them in Figure 5.

Simulations are made in an *E. coli* cell of $\sim 0.8 \times 10^{-3}\,\mu m^3$. This cell is represented by a single voxel with a lattice length of 0.8974 μm. There are 10 main species involved in the networks:

- RNA polymerase (P). In all simulations, the initial value for P is 3600 molecules (Link *et al*, 1997; Shepherd *et al*, 2001; Mooney and Landick, 2003)
- Plasmid expressing TetR, with the DNA segment of interest divided in two parts: the 'activator' part (A), which corresponds to the promoter (including any regulatory region), and the *tetR* gene (B)
- Plasmid expressing GFP, with the DNA segment of interest divided in two parts: the 'activator' part (C), which corresponds to the promoter (including any regulatory region), and the *gfp* gene (D)
- Chromosomal *E. coli* promoters, which are considered to be the same for simplicity (Z)
- Chromosomal *E. coli* genes/operons, which are considered to be the same for simplicity (Y)
- TetR mRNA (M)
- GFP mRNA (N)
- TetR protein. TetR is biologically active as a dimmer (Hillen and Berens, 1994). As TetR has an exceptionally high dimerization equilibrium constant (Backes *et al*, 1997), it is safe to assume that it will be only in the dimer form, even at low concentrations, and thus dimerization is not explicitly modelled. Therefore, for simplicity, it is considered that the product of the RNA transcript M is the biologically active species.
- GFP protein.
- aTc is modelled to bind with the same affinity to both free TetR and TetR–DNA complexes, resulting in preventing DNA binding or releasing DNA, respectively. As two molecules of aTc can bind to a TetR dimer, the stepwise binding of the aTc molecules to either free TetR (reactions (22) and (23)) or DNA-bound TetR (reactions (12), (13), (27) and (28)) has been explicitly modelled (see Figure 5).

For the sake of simplicity, the following assumptions were made:

- The whole process starting from the closed promoter–polymerase complex to actual transcription of the gene is modelled as one reaction with a rate constant k_{in}, which is considered to be the same for all promoters (reactions (2), (7) and (18)) (see Figure 5).
- The rate constants for the dissociation of promoter–polymerase complex are the same for all promoters. Thus, as k_{in} is also the same, differences in promoter strengths are modelled only by changing the k_{on} for the formation of the promoter–polymerase complex.
- As the length of the *tetR* and *gfp* genes is approximately the same, the rate constants of transcription, translation and RNA degradation are the same for them.
- As the half-life of TetR (Becskei and Serrano, 2000) and GFP (Andersen *et al*, 1998) exceed by far the time of cell division, it can be assumed that the degradation rate constants are equal and correspond to a half-life equal to the time of cell division as measured from the experiments in this study (degT″ rate='3.85e−4', degG″ rate='5.8e−4').
- Degradation of TetR is the same regardless of the number of aTc molecules bound to it.
- The rates of M/N degradation and TetR/GFP production ensure an RNA lifetime of around 3 min and that one copy of RNA produce around 20 copies of TetR/GFP protein before it is degraded.
- Formation of complex with one molecule of aTc reduces the repressor's binding rate constant to A from $k_{off\_T1}=10^{-5}\,s^{-1}$ to $k_{off\_T2}=0.001\,s^{-1}$ and with two molecules to $k_{off\_T3}=100\,s^{-1}$, based on the respective equilibrium constants (Lederer *et al*, 1995) and assuming that k_{on} is the same in all cases.
- When considering that plasmid numbers can fluctuate, we add or eliminate plasmids in a random fashion. Molecules attached to existing plasmids are released when the plasmid disappears.

All simulations followed the evolution of the different species for different aTc concentrations for 1 day (86 400 s)

Network 1

In the *E. coli* cell, there is only one type of plasmid, the one expressing TetR-GFP, with copy number 4 (thus A=4). TetR-GFP has the ability to repress its own production by competing with the RNA polymerase for binding to promoter A.

Network 2

In the *E. coli* cell, there are two types of plasmids: the one as in network 1 with A=4 and a plasmid that expresses GFP from the TetR-regulated promoter C, with a copy number 60 (thus C=60). The regulated promoter in both plasmids is the same and is repressed by TetR; so apart from the copy number, the values for the rate constants are the same for reactions involving A and C (Table I).

Network 3

It is the same as network 2 with the difference that TetR cannot repress its own transcription. Therefore, in this model, the rate constants for reactions involving A and C are different (Table I).

Acknowledgements

We thank Professor Bujard for providing plasmids pZE21-MCS-1, pZE12-luc and pZS*24-MCS-1 and strain DH5αZ1. We also thank Andy Riddell at the EMBL core facilities for his help with the flow cytometry experiments. This project was partly supported by EC grants LSHG-CT-2004-503568 and LSHG-CT-2003-505520.

References

Ander M, Beltrao P, Di Ventura B, Ferkinghoff-Borg J, Foglierini M, Kaplan A, Lemerle C, Tomas-Oliveira I, Serrano L (2004) SmartCell, a framework to simulate cellular processes that combines stochastic approximation with diffusion and localisation: analysis of simple networks. *Systems Biol* **1:** 129–138

Andersen JB, Sternberg C, Poulsen LK, Bjorn SP, Givskov M, Molin S (1998) New unstable variants of green fluorescent protein for studies of transient gene expression in bacteria. *Appl Environ Microbiol* **64:** 2240–2246

Austin DW, Allen MS, McCollum JM, Dar RD, Wilgus JR, Sayler GS, Samatova NF, Cox CD, Simpson ML (2006) Gene network shaping of inherent noise spectra. *Nature* **439:** 608–611

Backes H, Berens C, Helbl V, Walter S, Schmid FX, Hillen W (1997) Combinations of the alpha-helix-turn-alpha-helix motif of TetR with respective residues from LacI or 434Cro: DNA recognition, inducer binding, and urea-dependent denaturation. *Biochemistry* **36:** 5311–5322

Becskei A, Serrano L (2000) Engineering stability in gene networks by autoregulation. *Nature* **405:** 590–593

Becskei A, Seraphin B, Serrano L (2001) Positive feedback in eukaryotic gene networks: cell differentiation by graded to binary response conversion. *EMBO J* **20:** 2528–2535

Blake WJ, Kaern M, Cantor CR, Collins JJ (2003) Noise in eukaryotic gene expression. *Nature* **422:** 633–637

Chen L, Wang R, Zhou T, Aihara K (2005) Noise-induced cooperative behavior in a multicell system. *Bioinformatics* **21:** 2722–2729

Degenkolb J, Takahashi M, Ellestad GA, Hillen W (1991) Structural requirements of tetracycline–Tet repressor interaction: determination of equilibrium binding constants for tetracycline analogs with the Tet repressor. *Antimicrob Agents Chemother* **35:** 1591–1595

Elf J, Doncic A, Ehrenberg M (2003) Mesoscopic reaction–diffusion in intracellular signaling. *SPIE: Fluctuations Noise Biol Biophys Biomed Systems* **5110:** 114–124

Elf J, Ehrenberg M (2004) Spontaneous separation of bi-stable biochemical systems into spatial domains of opposite phases. *Systems Biol* **1:** 230–236

Elowitz MB, Levine AJ, Siggia ED, Swain PS (2002) Stochastic gene expression in a single cell. *Science* **297:** 1183–1186

Gardner TS, Cantor CR, Collins JJ (2000) Construction of a genetic toggle switch in *Escherichia coli*. *Nature* **403:** 339–342

Gibson MA, Bruck J (2000) Efficient exact stochastic simulation of chemical systems with many species and many channels. *J Phys Chem A* **104:** 1876–1889

Gillespie DT (1977) Exact stochastic simulation of coupled chemical reactions. *J Phys Chem* **81:** 2340–2361

Hattne J, Fange D, Elf J (2005) Stochastic reaction–diffusion simulation with MesoRD. *Bioinformatics* **21:** 2923–2924

Hillen W, Berens C (1994) Mechanisms underlying expression of Tn10 encoded tetracycline resistance. *Annu Rev Microbiol* **48:** 345–369

Hooshangi S, Thiberge S, Weiss R (2005) Ultrasensitivity and noise propagation in a synthetic transcriptional cascade. *Proc Natl Acad Sci USA* **102:** 3581–3586

Kepler TB, Elston TC (2001) Stochasticity in transcriptional regulation: origins, consequences, and mathematical representations. *Biophys J* **81:** 3116–3136

Lederer T, Takahashi M, Hillen W (1995) Thermodynamic analysis of tetracycline-mediated induction of Tet repressor by a quantitative methylation protection assay. *Anal Biochem* **232:** 190–196

Link AJ, Robison K, Church GM (1997) Comparing the predicted and observed properties of proteins encoded in the genome of *Escherichia coli* K-12. *Electrophoresis* **18:** 1259–1313

Lutz R, Bujard H (1997) Independent and tight regulation of transcriptional units in *Escherichia coli* via the LacR/O, the TetR/O and AraC/I1-I2 regulatory elements. *Nucleic Acids Res* **25:** 1203–1210

Mooney RA, Landick R (2003) Tethering sigma70 to RNA polymerase reveals high *in vivo* activity of sigma factors and sigma70-dependent pausing at promoter-distal locations. *Genes Dev* **17:** 2839–2851

Oliva B, Gordon G, McNicholas P, Ellestad G, Chopra I (1992) Evidence that tetracycline analogs whose primary target is not the bacterial ribosome cause lysis of *Escherichia coli*. *Antimicrob Agents Chemother* **36:** 913–919

Ozbudak EM, Thattai M, Kurtser I, Grossman AD, van Oudenaarden A (2002) Regulation of noise in the expression of a single gene. *Nat Genet* **31:** 69–73

Paulsson J (2004) Summing up the noise in gene networks. *Nature* **427:** 415–418

Pedraza JM, van Oudenaarden A (2005) Noise propagation in gene networks. *Science* **307:** 1965–1969

Raser JM, O'Shea EK (2004) Control of stochasticity in eukaryotic gene expression. *Science* **304:** 1811–1814

Savageau MA (1974) Comparison of classical and autogenous systems of regulation in inducible operons. *Nature* **252:** 546–549

Selinger DW, Cheung KJ, Mei R, Johansson EM, Richmond CS, Blattner FR, Lockhart DJ, Church GM (2000) RNA expression analysis using a 30 base pair resolution *Escherichia coli* genome array. *Nat Biotechnol* **18:** 1262–1268

Shepherd N, Dennis P, Bremer H (2001) Cytoplasmic RNA polymerase in *Escherichia coli*. *J Bacteriol* **183:** 2527–2534

Simpson ML, Cox CD, Sayler GS (2003) Frequency domain analysis of noise in autoregulated gene circuits. *Proc Natl Acad Sci USA* **100:** 4551–4556

Stundzia AB, Lumsden CJ (1996) Stochastic simulation of coupled reaction–diffusion processes. *J Comput Phys* **127:** 196–207

Swain PS, Elowitz MB, Siggia ED (2002) Intrinsic and extrinsic contributions to stochasticity in gene expression. *Proc Natl Acad Sci USA* **99:** 12795–12800

Thieffry D, Huerta AM, Perez-Rueda E, Collado-Vides J (1998) From specific gene regulation to genomic networks: a global analysis of transcriptional regulation in *Escherichia coli*. *BioEssays* **20:** 433–440

Vilar JM, Saiz L (2005) DNA looping in gene regulation: from the assembly of macromolecular complexes to the control of transcriptional noise. *Curr Opin Genet Dev* **15:** 136–144

Zacharias DA, Violin JD, Newton AC, Tsien RY (2002) Partitioning of lipid-modified monomeric GFPs into membrane microdomains of live cells. *Science* **296:** 913–916